GERDA

Progress Report to the LNGS Scientific Committee

LNGS-EXP 33/05 add. 5/07

October 2007

A.M. Bakalyarov [h], M. Balata [a], I. Barabanov [f], L. Baudis [m], C. Bauer [c], E. Bellotti [e], S. Belogurov [f,g], S. T. Belyaev [h], M. Barnabe-Heider [c], A. Bettini [j], L. Bezrukov [f], V. Brudanin [b], D. Budjas [c], A. Caldwell [i], C. Cattadori [a,e], O. Chkvorets [c], E. V. Demidova [g], A. Di Vacri [a], V. Egorov [b], A. Ferella [m], A. Gangapshev [f], J. Gasparro [l], P. Grabmayr [k], G. Y. Grigoriev [h], K. N. Gusev [h], V. Gurentsov [f], W. Hampel [c], M. Heisel [c], G. Heusser [c], W. Hofmann [c], M. Hult [l], L.V. Inzhechik [h], J. Janicsko [i], M. Jelen [i], J. Jochum [k], M. Junker [a], S. Katulina [b], J. Kiko [c], I.V. Kirpichnikov [g], A. Klimenko [b,f], M. Knapp [k], K.T. Knoepfle [c], O. Kochetov [b], V.N. Kornoukhov [f,g], K. Kroeninger [i], V. Kusminov [f], M. Laubenstein [a,e], V.I. Lebedev [h], D. Lenz [i], M. Lindner [c], J. Liu [i], X. Liu [i], B. Majorovits [i], G. Marissens [l], I. Nemchenok [b], L. Niedermeier [k], J. Oehm [c], L. Pandola [a], P. Peiffer [c], A. Pullia [e], F. Ritter [k], C. Rossi Alvarez [j], V. Sandukovsky [b], S. Schoenert [c], J. Schreiner [c], J. Schubert [i], U. Schwan [c], B. Schwingenheuer [c], M. Shirchenko [h], H. Simgen [c], N. Smale [c], A. Smolnikov [b,f], F. Stelzer [i], A.V. Tikhomirov [h], C. Tomei [a], U. Trunk [c], C.A. Ur [j], A.A. Vasenko [g], S.Vasiliev [b,f], M. Wojcik [d], E. Yanovich [f], J. Yurkowski [b], S.V. Zhukov [h], E. Zocca [e], G. Zuzel[c]

[a] INFN Laboratori Nazionali del Gran Sasso, Assergi, Italy
[b] Joint Institute for Nuclear Research, Dubna, Russia
[c] Max-Planck-Institut für Kernphysik, Heidelberg, Germany
[d] Institute of Physics, Jagellonian University, Cracow, Poland
[e] Università di Milano Bicocca e INFN Milano, Milano, Italy
[f] Institute for Nuclear Research of the Russian Academy of Sciences, Moscow, Russia
[g] Institute for Theoretical and Experimental Physics, Moscow, Russia
[h] Russian Research Center Kurchatov Institute, Moscow, Russia
[i] Max-Planck-Institut für Physik, München, Germany
[j] Dipartimento di Fisica dell'Università di Padova e INFN Padova, Padova, Italy
[k] Physikalisches Institut, Universität Tübingen, Germany
[l] Institute for Reference Materials and Measurements, Geel, Belgium
[m] Physik Institut der Universität Zürich, Zürich, Switzerland

Spokesperson: S. Schönert,
(Stefan.Schoenert@mpi-hd.mpg.de)
Co-Spokesperson: C. Cattadori
(Carla.Cattadori@lngs.infn.it)
Technical Coordinator: K.T. Knöpfle
(Karl-Tasso.Knoepfle@mpi-hd.mpg.de)

URL: http://www.mpi-hd.mpg.de/GERDA/reportsLNGS/gerda-lngs-sc-oct07.pdf

Contents

1 Executive summary **4**

2 Phase I detectors **7**
2.1 Study of leakage currents . . . 7
2.2 Processing of Phase I detectors . . . 8
2.3 Low-background test stand LArGe . . . 9

3 Phase II detectors **9**
3.1 Prototype tests . . . 9
3.2 Production of Phase II detectors . . . 10

4 Front-End electronics **13**
4.1 Status of F-CSA104 preamplifier . . . 13
4.2 Status of PZ preamplifiers . . . 13
4.3 Cables and HV connectors . . . 15

5 Data acquisition **15**

6 Cryogenic vessel and infrastructure **17**

7 Water tank and infrastructures **20**

8 Muon veto **21**
8.1 Cherenkov veto . . . 21
8.2 Plastic veto . . . 22

9 Infrastructure on top of the tank **22**
9.1 Clean room . . . 22
9.2 Lock system . . . 23

10 Monte carlo simulations and background studies **25**

11 Material screening **27**
11.1 ^{222}Rn emanation measurements . . . 27
11.2 ^{222}Rn in argon . . . 27
11.3 γ ray screening . . . 28
11.4 ICPMS measurements . . . 29
11.5 Low-level instrumentation . . . 30
11.6 Radon monitoring . . . 31

1 Executive summary

This report summarizes the progress of the GERDA collaboration accomplished since the last meeting of the LNGS Scientific Committee in April 2007. The most relevant issues are given in a concise form in the executive summary. A more detailed description can be found in the respective sections.

- **Completion of safety audit:** The LNGS Prevention and Protection Service (SPP) completed the GERDA safety audit with a final document dated 18 June 2007. Subsequently, the director of the LNGS approved the experimental setup and its safety concept, and authorized the GERDA collaboration to install the GERDA experiment in the Gran Sasso underground laboratory.

- **Phase I detectors:** The detector leakage current (LC) in response to gamma radiation has been studied extensively with the Phase I prototype detector (^{nat}Ge). After nine months of continuous operations in liquid argon, the detector assembly exhibits a LC of approximately 25 pA, similar to the value measured at the beginning of the tests in February. Higher LC values were observed following extensive irradiation. However, the LC increase is reversible and the values returned to their initial values following irradiation with switched off bias voltage. The gamma induced LC increase is most likely related to charge collection on the insulating passivation layer. Additional measurements to study the effects are under preparation. All enriched (8 crystals, 17.9 kg) and non-enriched (6 crystals, 15 kg) detectors for Phase I have been processed at the manufacturer. The last work steps will be done after the final definition of the passivation layer. The cryostat for the low-background test stand LARGE in the GERDA underground Detector Laboratory (GDL) is close to completion. Delivery to Gran Sasso is planned prior to the end of the year.

- **Phase II detectors:** A second 18-fold segmented prototype detector is ready for delivery. A third 19-fold segmented detector has been ordered with a disk like segment 5 mm thick at one end to understand the response of the detector near these surfaces. R&D efforts are currently underway with PPM Pure Metals GmbH for test of the purification procedures. First successful tests of the purification of GeO_2 have been performed with depleted germanium. The GeO_2 was first reduced to Ge and then zone refined. No isotopic dilution was observed. The chemical purity of the material was typically at the detection limit of the mass spectrometry. A R&D contract has been signed with the Institut für Kristallzüchtung (IKZ) in Berlin for crystal production. A timetable has been defined for producing detector grade crystals within a 15 month period. The work has started October 2007.

- **Front-End electronics:** Major efforts have been devoted to tests of the F-CSA104 CMOS ASIC preamplifier and on the development of a double layer test printed circuit board (PCB) for the PZ-0 and PZ-1 CMOS ASIC preamplifiers. Several prototype preamplifiers have been prepared for tests with crystals. Sample high voltage (HV) connectors suitable for operation in Ar gas have been produced and the radioactive impurities of various HV and signal cables have been measured.

- **Cryogenic vessel:** The delivery of the cryostat has been delayed and is now scheduled for February 2008. The welding procedures have passed the certification requirements at liquid nitrogen temperature. The copper plates for the internal shielding have been completed and delivered to LNGS. The tender draft for the cryogenic infrastructure has been prepared and is under discussion with external experts. Instrumentation like radon tight valves have been identified.

- **Water tank:** The anchorage points for the fixation of the cryostat have been mounted in the concrete basement of hall A in June 2007. Subsequently the bottom plate of the water tank (WT) has been mounted in July. The WT construction will continue after the delivery of the cryostat.

- **Muon veto system:** Encapsulated photomultiplier (PMT) prototype assemblies have sustained extensive tests for water tightness under elevated pressures. The electronic performance of the final PMT assembly has been tested. Ten plastic scintillator panels have been prepared and are ready for shipping. The DAQ and trigger logic for the muon veto has been defined and tests with the system are under preparation.

- **Clean room and lock system:** The clean room is presently in the tendering process. The winning company will be determined in November. Main parts or mock-ups of the lock system, as the inner rail system, the linear pulley system, the shutters are under test. The insertion of mock-up strings into liquid argon has been successfully tested.

- **Monte Carlo simulations:** The Monte Carlo activities have been closely related to the Phase I prototype detector tests, the LArGe test stand, the Phase II detector response, the muon veto response and material screening. In collaboration with Majorana the Monte Carlo groups have started the development of the MGDO (Majorana–Gerda data object) for interfacing the Geant4 based event simulation with external software packages to simulate the pulse shapes of the events.

- **Material screening:** Radon emanation measurements have been carried out for many different materials of the lock system, to identify the most suited cryogenic valves, to investigate adsorber materials and cable candidates. The search for argon with low initial radon concentrations and the study of the performance of liquid phase adsorbtion columns has been continued. Most of the γ screening had to be carried out at Irmm Geel and Lngs Assergi because the low-level laboratory at MPIK is currently renovated and the HPGe detectors at INR Baksan had to be repaired. A large fraction of the measurement time was dedicated to the assay of small parts as cables and miniature electrical connectors (pins). ICPMS measurements of polymeric substrates for cables and printed circuit boards (PCB) have been done. Several new low-level instruments are under preparation or have been already installed. The origin of the reported contamination of the GeMPI-iii and iv has been identified. One detector has been dismounted and acid cleaned part by part. Preliminary results indicate a reduction by a factor of four. Further steps are needed to reach the design sensitivity. The new radon monitor is currently under test. A high voltage of 50 kV could be reached.

- **Personnel:** The group of Laura Baudis from University Zürich joined the collaboration this summer. The main responsibility of the group concerns the energy calibration of Gerda. Contribution to Phase II detectors are contingent on the available funding in the future. The collaboration has been successful to hire a project engineer for on-site coordination and supervision of the Gerda experiment.

- **Schedule:** The schedule of the experiment is currently driven by the delivery time of the cryostat. The production delay has shifted the schedule by approximately four months. The completion of the hardware installation is now projected for the beginning of 2009.

2 Phase I detectors

Gerda Phase I will operate 17.9 kg of enriched and 15 kg of non-enriched detectors , which were used in the past in the HdM and Igex experiments, and in the Genius Test Facility (GTF). As described in earlier reports, the preparation of Phase I detectors has been broken down into five work packages (WP). WP1 concerns the installation of the Gerda Underground Detector Laboratory (Gdl), WP2 the testing and characterization of the HdM and Igex detectors prior to dismounting, WP3 the testing of Phase I prototype detector assemblies, WP4 the dismounting and processing of Phase I crystals, and WP5 the construction and operating of the low-background test stand LArGe in the Gdl inclusive testing of Phase I detector assemblies. Pulse shape discrimination studies of liquid argon scintillation light for background identification are being pursued in WP5. The main activities during the period under report concerned the tests of the Phase I prototype detector in the Gdl, the refurbishment of Phase I detectors and the preparation of the LarGe test stand. Studies of pulse shape properties of liquid argon scintillation for background identification and reduction complemented the activities.

2.1 Study of leakage currents

The Phase I prototype detector assembly has been operated continuously through 2006 and 2007. In total 44 thermal cycles have been performed. During this period, the passivation layer has been refurbished twice, the first time in August 2006 and the second time in January 2007. Measurements in conjunction with front-end electronics tests during autumn 2006 gave first indications that continuous exposure to gamma radiation of the detector assembly immersed in liquid argon can lead to an increase of the leakage current (LC).

A new series of measurements with the Phase I prototype detector assembly commenced in February 2007. The detector was irradiated with a 44 kBq ^{60}Co gamma source with different source–crystal distances, exposure times, electric field configurations and bias voltages values. Dedicated irradiations with the high voltage switched off complemented the measurements. The goals of these experiments were to investigate the origin of the gamma induced leakage current, to quantify the LC increase with respect to the energy deposition in the liquid argon, and to develop mitigation strategies. Detailed Monte Carlo simulations of energy deposition and electric field modeling of the crystal and the holder complemented the experiments.

After nine months of continuous operations in liquid argon, the detector assembly exhibits a LC of about 25 pA, similar to the value measured at the beginning in February. Higher values were observed following extensive irradiation, however, it turned out that irradiation with high the voltage switched off reduced the initial LC values to its prior irradiation values.

Though the measurements are still ongoing, the experimental details and results are documented in a preliminary Gerda Scientific and Technical Report (GSTR) [1]. Models to explain the observations and mitigation strategies are summarized in two GSTR's [2, 3]. The most plausible explanation is that charges created by gamma interactions in the liquid argon volume close by the borehole side of the crystal are collected on the insulating passivation layer. This accumulation of charges changes the electronic properties of the insulator-semiconductor system which leads to an increased LC. Neutralizing or removing the charges e.g. by UV irradiation from the liquid argon scintillation light reduces the LC current to its initial values. Operating the diode with the passivation layer covered with an PTFE/Cu/PTFE structure showed a strong reduction of the gamma induced increase of LC.

Two GTF crystals with modified passivation structures have been prepared in October by Canberra, Olen. The objective of these measurements is to further investigate the origin of the effect and to minimize, or even avoid completely gamma induced LC. Measurements with these crystals will start beginning of November.

It is worth to mention that based on our experimental findings, Phase I of GERDA can be carried out even with the present passivation configuration as realized in the prototype tests. Even if a weekly energy calibration with gamma sources were to be carried out, the cumulative increase of leakage current is expected to be negligible.

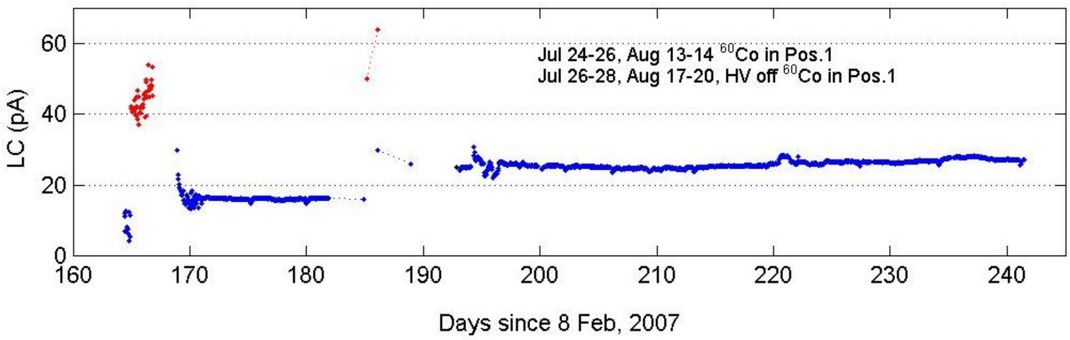

Figure 1: Leakage current (LC) values of the Phase I prototype detector in liquid argon in the period July through October 2007. The LC values during irradiation exhibits a step-like increase (red points) with $\Delta I \approx 35$ pA corresponding to the current of the charge carrier produced by γ radiation in the bulk of the diode. Small 'dips' of the LC curve are related to the refilling of the dewar with liquid argon.

2.2 Processing of Phase I detectors

As described in previous reports to the LNGS SC, two detectors, ANG1 and RG3, have been fully processed in 2006. In October 2007, two non-enriched GTF crystals have been processed for testing the impact of the passivation layer geometry on the LC as discussed above. The remaining six enriched and four non-enriched crystals have been machined and lithium drifted. All crystals are stored deep underground to avoid cosmogenic activation.

Given the observation of the radiation induced LC increase early this year, we decided to await the completion of the ongoing tests in order to define the optimal configuration of the passivation layer. All crystals, including the non-enriched ones are stored in vaccuum containers deep underground to avoid cosmogenic activations.

2.3 Low-background test stand LArGe

The lock system, the shielding and the connecting lines of the cryogenic lines of the low-background detector test stand (LArGe) are available now. Capacity problems at the cryostat manufacturer delayed the installation of the system. The main welding work has been completed during September, and the cryostat is currently prepared for surface cleaning (electro-polishing for the inner vessel and pickling and passivation for the other shells) and final assembly at the manufacturer. After completion of first cryogenic tests, it will be delivered to LNGS and the integration of the system will start subsequently. Fig. 2 shows the inner tank including the stainless steel heat exchanger integrated in the neck as of September 2007.

Figure 2: Inner shell of the LArGe copper cryostat with the integrated heat exchanger.

3 Phase II detectors

3.1 Prototype tests

The successful test of the first 18–fold segmented n–type prototype produced by Canberra-France was described in a previous report. Several papers describing the performance of this detector have been published or are in the publishing process [4]. A second prototype 18–fold segmented detector has been ordered from Canberra, and is ready for delivery. A third 19-fold segmented detector has been ordered with a disk like segment 5 mm thick at one end to understand the response of the detector near these surfaces. We expect to operate the first two detectors in a final phase II string setup by early next year. A special test cryostat to facilitate this is under construction at the Max Planck Institute in Munich.

This cryostat is a prototype of the test cryostat to be installed in the GERDA clean-room at the LNGS.

3.2 Production of Phase II detectors

The enriched Ge for the Phase II detectors has been procured and is in underground storage while we investigate purification and crystal growing options. R&D efforts are currently underway with PPM Pure Metals GmbH (PPM), Langelsheim, for tests of the purification procedures, and with the Institut für Kristallzüchtung (IKZ) in Berlin for crystal production.

Purification First successful tests of the purification of GeO_2 have been performed at PPM Pure Metals. Depleted Ge (<1 % ^{76}Ge) in the form of GeO_2 produced at the Electrochemical Plant in Siberia (from the 'waste' of the enrichment procedure) was used. The GeO_2 was first reduced to Ge in a reduction furnace, and then zone refined. Detailed measurements were performed on the input sample, samples after reduction and samples after zone refining to look for signs of isotopic dilution and to measure chemical and electronic impurities. The results are summarized in Tables 1 and 2.

	Ge1a	**Ge1b**	**Ge2b**	**Ge3b**	**Ge4b**	**Ge_i1**	**Ge_i3**	**Ge_i4**	**Ge n**
70	22.8	22.7	22.8	22.8	22.8	22,74	22,75	22,70	21.2
72	30.1	30.0	30.00	30.00	30.00	30,07	30,05	30,08	27.8
73	8.32	8.30	8.33	8.33	8.32	8,32	8,30	8,29	7.75
74	38.2	38.4	38.3	38.3	38.3	38,27	38,30	38,34	35.9
76	0.59	0.60	0.59	0.59	0.60	0,60	0,60	0,59	7.35

Table 1: Isotopic composition in % of Ge after successive steps of purification. Samples Ge1a and Ge1b are depleted GeO_2, samples Ge2b - Ge4b are depleted Ge metal after reduction, samples Ge_i1 - Ge_i4 are Ge metal after zone-refinement at PPM Pure Metals, sample Ge n - sample of natural germanium

No sign of isotopic dilution was found. The chemical purity of the material was typically at the detection limit of the mass spectroscopy. Some positive identification of impurities was possible for Fluorine, Aluminum, Silicon and Iron, amounting to 0.5 ppm . The impact of electrically active impurities can be directly measured via resistivity measurements. Resistivity measurements were performed at room temperature at the PPM, and reproduced at the MPI. Further measurements at the MPI at liquid nitrogen (LN) temperature are shown in Fig. 3, and give values around 400 Ωcm. These measurements were performed on polycrystalling material, such that only a lower limit of 10^{11} cm^{-3} on the net electrically active impurity level can be given. The resistivity measurements, along with temperature dependent Hall effect measurements and photothermal ionization spectroscopy measurements will be performed on monocrystals produced from the same samples to accurately determine the net impurity concentration as well as to identify individual impurities.

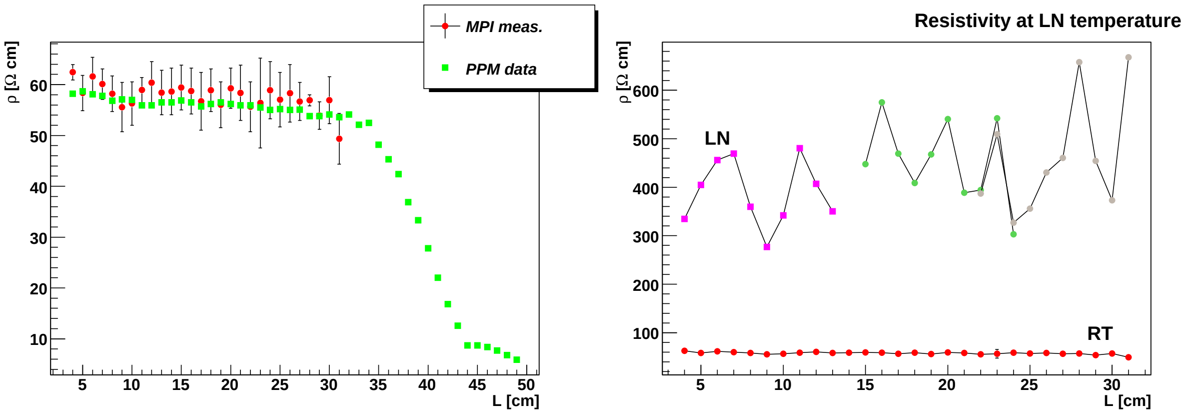

Figure 3: Resistivity at room temperature (left) and at LN temperature (right)

The yield of high resistivity material from the zone refining was about 60 % per step. Tails from three batches were further processed, and again a yield of 60 % was achieved for high resistivity material. Not enough material was at hand to attempt a third zone refining step.

A second series of tests has been started at the PPM with the goal to investigate the yield which can be achieved in the purification, and to set up a protocol for the reduction and zone refinement which minimizes the time the material is subjected to cosmogenic activation. A storage facility in a mine near the PPM has been located where the material can be placed between steps. Enough GeO_2 has been provided to the PPM so that three passes of zone refining should be possible, allowing us to estimate the ultimate yield from the purification process.

To reach the quality material needed for crystal pulling, at least one order of magnitude improvement is needed in the electrically active impurity levels. We are currently defining the steps which will be necessary to reach the needed impurity levels (materials used for boats, coatings, atmosphere for refinement, speed of the melted zone, number of passes, etc.) and foresee a third test with the PPM to demonstrate that this high purity can be reached. Once this is demonstrated, we would be in a position to perform the purification of our enriched Ge.

Crystal Pulling A dedicated Czochralski crystal puller has been set up at the IKZ for crystal pulling tests. A R&D contract has been signed, and a timetable defined for producing detector grade crystals within a 15 month period. The R&D program starts this October. Initially, 6N natural Ge will be used and a reliable and reproducible method for pulling single crystals of the desired dimensions (approximately 80 mm diameter and 70 mm length) will be established. Once a reliable procedure has been set up, high purity material will be used as input, and it will be determined if the crystal growing conditions at the IKZ are suitable for the production of the very high purity crystals needed for Ge detectors. The parameters of the crystal (dislocation density, impurity density, etc.)

required for the production of a Ge detector have been defined in conjunction with Canberra-France. Once these conditions on the crystal properties are met, we will attempt to produce functioning detectors. These tests will all be performed with natural or depleted Ge. If the IKZ is successful, then we plan to proceed and grow crystals with the enriched Ge. The funding for the development of the purification and crystal pulling procedures is in place. The funding for the crystal and detector production for the enriched material will need to be acquired once the procedures and costs are determined.

Element	ppm weight	Element	ppm weight	Element	ppm weight
H	ND	Zn	<0.02	Pr	<0.05
Li	<0.001	Ga	<0.01	Nd	<0.2
Be	<0.001	Ge	(matrix)	Sm	<0.1
B	<0.001	As	<0.1	Eu	<0.04
C	ND	Se	<0.2	Gd	<0.2
N	ND	Br	<0.1	Tb	<0.1
O	ND	Rb	<0.1	Dy	<0.3
F	0.4	Sr	<0.2	Ho	<0.06
Na	<0.02	Y	<0.1	Er	<0.04
Mg	<0.01	Zr	<0.2	Tm	<0.05
Al	0.03	Nb	<0.1	Yb	<0.2
Si	0.02	Mo	<0.3	Lu	<0.1
P	<0.005	Ru	<0.1	Hf	<0.2
S	0.04	Rh	<0.05	*Ta	ND
Cl	ND	Pd	<0.3	W	<0.2
K	<0.02	Ag	<0.05	Re	<0.1
Ca	<0.01	Cd	<0.2	Os	<0.4
Sc	<0.01	In	<0.05	Ir	<0.2
Ti	<0.01	Sn	<0.1	Pt	<0.2
V	<0.05	Sb	<0.05	Au	<0.1
Cr	<0.01	Te	<0.4	Hg	<0.3
Mn	<0.01	I	<0.05	Tl	<0.1
Fe	0.05	Cs	<0.1	Pb	<0.3
Co	<0.01	Ba	<0.2	Bi	<0.1
Ni	<0.05	La	<0.1	Th	<0.1
Cu	<0.02	Ce	<0.1	U	<0.1

Table 2: Sample **4.3**, ^{dep}Ge after zone refinement at PPM Pure Metal, *Ta is material of the ion source. These measurements are from spark source mass spectroscopy. The symbol ND indicates that this element was not measureable.

4 Front-End electronics

Major efforts of TG3 have been devoted to tests of the F-CSA104 CMOS ASIC preamplifier and on the development of a double layer test printed circuit board (PCB) for the PZ-0 and PZ-1 CMOS ASIC preamplifiers. Sample high voltage (HV) connectors suitable for operation in Ar gas have been produced and the radioactive impurities of various HV and signal cables have been measured. The following subsections provide more information about the respective activities.

4.1 Status of F-CSA104 preamplifier

The F-CSA104 is a fully integrated, low noise, differential, four channel preamplifier for GERDA which has been fabricated in 0.6 μm CMOS technology by XFab. It has been designed to have at cryogenic temperature an equivalent noise charge (ENC) of about $160\,e^-$ at $C_{input} = 30$ pF, a dynamic range of ±600 fC corresponding to ±11 MeV energy deposition in germanium, and a rise time of approximately 20 ns. Mounted on a flat Kapton cable, its performance has been extensively tested at room and LN temperatures. The differential receiver and shaping amplifier were operated at room temperature. The measured linearity and gain are satisfactory, and with optimized currents settings for the input transistor to minimize the common mode noise, the single channel ENC (without common mode subtraction) is found to be 270 e^- and 310 e^- at LN and room temperature, respectively, for $C_{input} = 35$ pF and $20\,\mu$s peak shaping time (270 e^- correspond to 2.6 keV FWHM in Ge). A F-CSA104 preamplifier has been operated at room temperature with a Ge detector but the resolution is still poor, about 6 keV FWHM.

4.2 Status of PZ preamplifiers

The integrated circuit named PZ-0 [5] [6] is designed for and produced by AMS in HV CMOS 0.8 μm CZX technology. It is extremely light and compact with a surface occupancy on silicon of only $366\times275\,\mu\text{m}^2$, and it takes advantage of a newly designed single-ended line-driver to drive a cable load of $50\,\Omega$. In this version the front-end FET as well as the feed-back components are discrete SMD components, while the first stage and line driver are fully integrated. It has been designed to satisfy the GERDA specifications, including operation at cryogenic temperatures. It exists in two versions which differ only in the value of the compensating capacitor at the amplifying node. The chip performances obtained at cryogenic temperatures at a test bench with capacitors at the input to simulate the detector are satisfactory and can be summarized as follows: 15 ns rise time, ENC of 110 e^- (T=77 K) for $C_{Det} = 15$ pF at $10\,\mu$s shaping time, driving a $50\,\Omega$ load with 10 m long cable. Sixteen chips and the respective PCBs are available. Two chips have been bonded in adequate miniaturized packages, mounted on the Cuflon PCB, and are ready to be tested with a detector (Fig. 4).

The integrated circuit named PZ-1 is produced by AMS in HV CMOS 0.8 μm CZX technology. It is fully integrated, apart from the feedback resistor. The input FET is a large

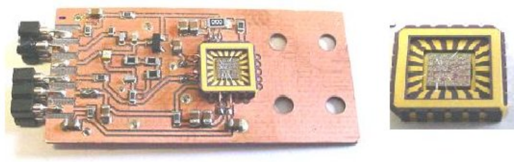

Figure 4: The PZ0 ASIC circuit mounted in ceramic package LCC20 (right) and in its package on a Cuflon PCB board (left).

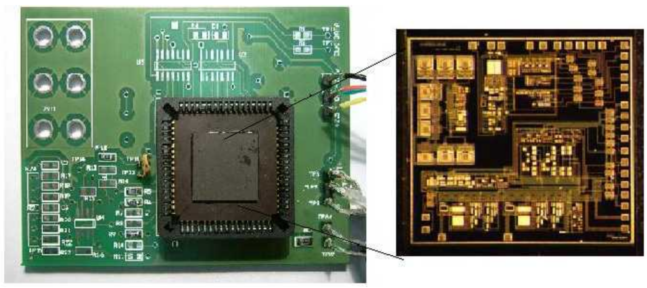

Figure 5: The PZ1 chip (right) mounted in the test package and on the test PCB (left). The discrete components are used to properly tune their values with *ad hoc* tests and will be integrated in the forthcoming production.

area newly developed low noise PMOS device. The ASIC consists of two separate parts: a very low noise preamplifier followed by a low noise fully differential amplifier (FDA). The amplifier takes advantage of an active reset circuit that can be used alternatively to the feedback resistor. Fine tuning and optimization of the main design parameters (MOS device channel widths and lengths, resistor and capacitor values) was performed by applying previously developed techniques to best trade-off between noise, power consumption, bandwidth and silicon die area, both at room and cryogenic temperature. Nonetheless, because of the inherent poor modeling reliability of MOS and passive elements at cryogenic temperature (e.g. MOS drain saturated current depending on increased voltage threshold and charge mobility with respect to ambient temperature), the front-end electronics has been designed so that the bias current of the fundamental elements can be tuned in real time by switching on or off a couple of parallel current generators controlled by digital signals. The DC gain of the preamplifier, the bandwidth and the bias output driver current of the FDA can be tuned in the same way. The fine tuning of the PZ-1 circuit was done both at room and LN temperatures; for this purpose it has been mounted in a suitable carrier and onto a double layer PCB (Fig 5).

The relevant obtained performances are: 25 ns rise time, ENC of 160 e^- (T=77 K) for C_{Det} = 33 pF at 12 μs shaping time, that are further reduced to 150 e^- when applying DPLMS filtering techniques. A new circuit layout is prepared for submission to the foundry on October 10. The new design integrates all the components that are external in the actual design whose values have been optimized in dedicated tests. Also a few samples of this circuit are bonded and mounted waiting to be tested with a detector.

An encapsulated Euroball detector (n-type) will be available by middle of October to compare the FE circuits under identical conditions. It is suitable for the PZ-1 and F-CSA104 circuits only which have been developed for both holes and electrons readout. The PZ-0 circuit, being developed for the readout of phase I detectors (p-type, holes readout) cannot be tested with this encapsulated detector. A second front-end electronic test stand has been built for testing the integration of the cold front-end electronics with a p-type detector. The cryostat holding the p-type crystal can be immersed in liquid nitrogen together with the externally mounted front-end electronics. The cryostat is has been successfully vaccuum tested, both at room and liquid nitrogen temperature. It will be equipped with a crystal within the next weeks.

4.3 Cables and HV connectors

Further candidates for signal and HV cables have been screened by γ-ray spectrometry. A good choice among micro-coaxial cables is now available. Table 3 list them together with the main technical specifications. Some of them have been tested in the lock and rail mock-up system. A couple of candidates exist also for HV cables. The low voltage cables needed to power the preamplifier has to be determined. Differential cables (in case the fully integrated circuit would be chosen) have not yet been fixed.

HV connectors for Ge detector and photomultiplier tube (PMT) biasing are in production in the INFN–PD electronic workshop. The technology of these HV connectors which are suitable for operation in a cryogenic Ar gas environment has been developed within the Icarus project.

	Coax	Impedence	Max V
Habia Teflon Subminiatur	yes	50Ω	-
Teledyne Reynolds Teflon coated	no	-	5 kV
Atlas Axon Subminiatur Kapton coated	yes	50Ω	-
Caburn 1-CC-0712 Kapton coated	yes	50Ω	5 kV
Caburn 1-CC-0710 Kapton coated	yes	$\approx 50\Omega$	2 kV

Table 3: Technical specifications of screened cables for Ge detector high voltage bias and signal readout.

5 Data acquisition

In the previous report the updated event format for the FADC system developed by INFN Padova and Milano has been discussed: for the energy measurement four samples with 10 ns spacing are summed and stored in FPGA memory while for the analysis of the rising edge of the detector pulse 512 samples taken with the full sampling frequency of 100 MHz are available. Due to the increased stored pulse length shaping times up to 20 μs are possible which lead to a reduction of the serial noise contribution by 10-20%.

The intrinsic noise performance of the FADC system (without input signal) is shown in Fig. 6. A signal–to–noise ratio is 72.3 dB, independent of an adjustable analog input offset. This corresponds to an effective number of bits (ENOB) of 11.7 which is better than the specified 10–11 bits needed for GERDA.

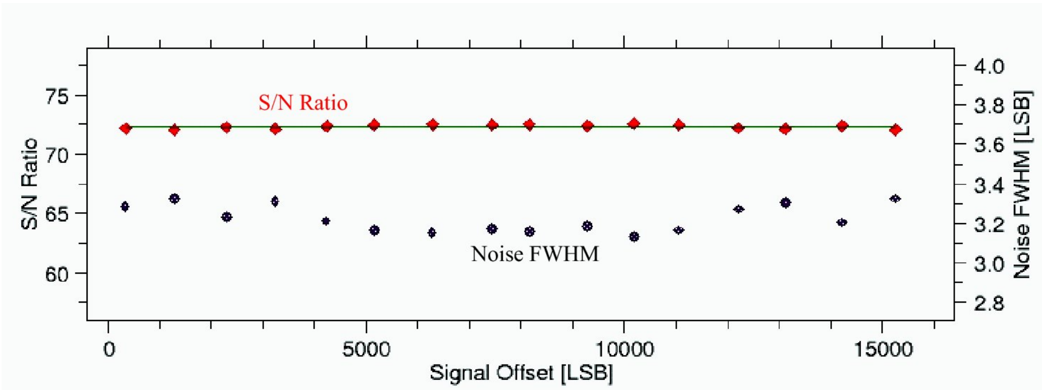

Figure 6: Signal–to–noise ratio and FWHM of the noise measured without any input signal for different signal offset values.

Also, the online/offline analysis program jSpecView has been updated by including additional analysis histograms, e.g. for signal rise time and fall time, by developing semi–automatic procedure for the iterative search for the best parameters of the moving window deconvolution calculation for the energy reconstruction, by the optimization of the Java code for execution speed, as well as by the implementation of a procedure for remote control and operation of the system. Details on the acquisition system, the GUI for its control and the analysis program can be found at the Web location **http://agata.pd.infn.it** under the link '*Local activities/Digital DAQ*'. The last version of the jSpecView program can be downloaded by following this link.

In the reporting period studies were performed on the muon veto performance. It is foreseen to digitize the muon PMTs with twelve SIS3301 FADC cards. Each card has 8 inputs with individual trigger thresholds but only one common trigger output which is the logical "OR" of all channels.

The random trigger rate of every PMT is expected to be up to 5 kHz. A veto which would require only one channel firing would hence cause a huge dead time. Instead, the coincidence of two or more PMTs has to be required for a veto. Since the trigger logic has only the OR of the hits from 8 channels available, only the coincidence of groups of PMTs can be formed by the logic.[1] Hence the grouping of channels has influence on the veto rate and efficiency.

[1]The trigger logic can be implemented on Xilinx FPGAs as discussed in the previous report.

The mapping of PMTs to the FADCs has been studied based on a detailed simulation of Cherencov light produced by muons, the propagation of the light through the water, and its arrival time at the PMTs. The goal has been to distribute those channels which will be hit by a muon to different FADCs. The coincidence of two or more FADCs will then register muons efficiently and the rate of random coincidences can be reduced.

Results for a good mapping are obtained for coincidences of 10 ns and 30 ns long trigger output signals from the FADCs and for the requirement of two to four cards triggering. The best performance is achieved for 30 ns long trigger signals and requiring the coincidence of 3 FADCs. The random rate is 13 Hz and the efficiency for muon detection is 99.5%. With this rate the hit pattern from the muon system together with a precise time stamp of 10 ns resolution can be saved to disk. The decision whether an event in a germanium detector is correlated with a muon passing through can be made in the offline analysis.

6 Cryogenic vessel and infrastructure

The delivery of the cryostat - being delayed by more than half a year - is expected now to be around mid of February 2008. The actual updated time schedule, Rev. 5 (Fig. 10), has been discussed on September 24 at Heidelberg with representatives of the manufacturing company who assured this plan to be now final.

One major reason for the delay was the very late delivery of the fourth vessel head on June 21 which needed repair (Fig. 7) because of welding imperfections (the other three heads were delivered in March). The procedure for this repair was certified in collaboration

Figure 7: Repair of bottom head of inner vessel at Antonius (7 June 07, left), and machining of supports of inner vessel head (September 07).

with the TÜV Nord in order to warrant optimum weld quality. Another reason for the delay were problems of the manufacturing company to acquire in time the needed welding certification according to AD2000. After several attempts, a procedure has been found which yielded for the low temperture notch impact energy a very good value of 120 J which is almost four times higher than required by AD2000 (the corresponding value of the base material is typical 200 J at 77K!).

Figure 8: September 07: Machining of the 12 m long stainless steel sheets for the cylindrical shell of the cryostat: bevelling (left), and rolling (right).

Figure 9: 11 Jun 2007: Assembly of a segment for the internal copper shield (left) and preparation of vacuum-packaging for assembled segment (right).

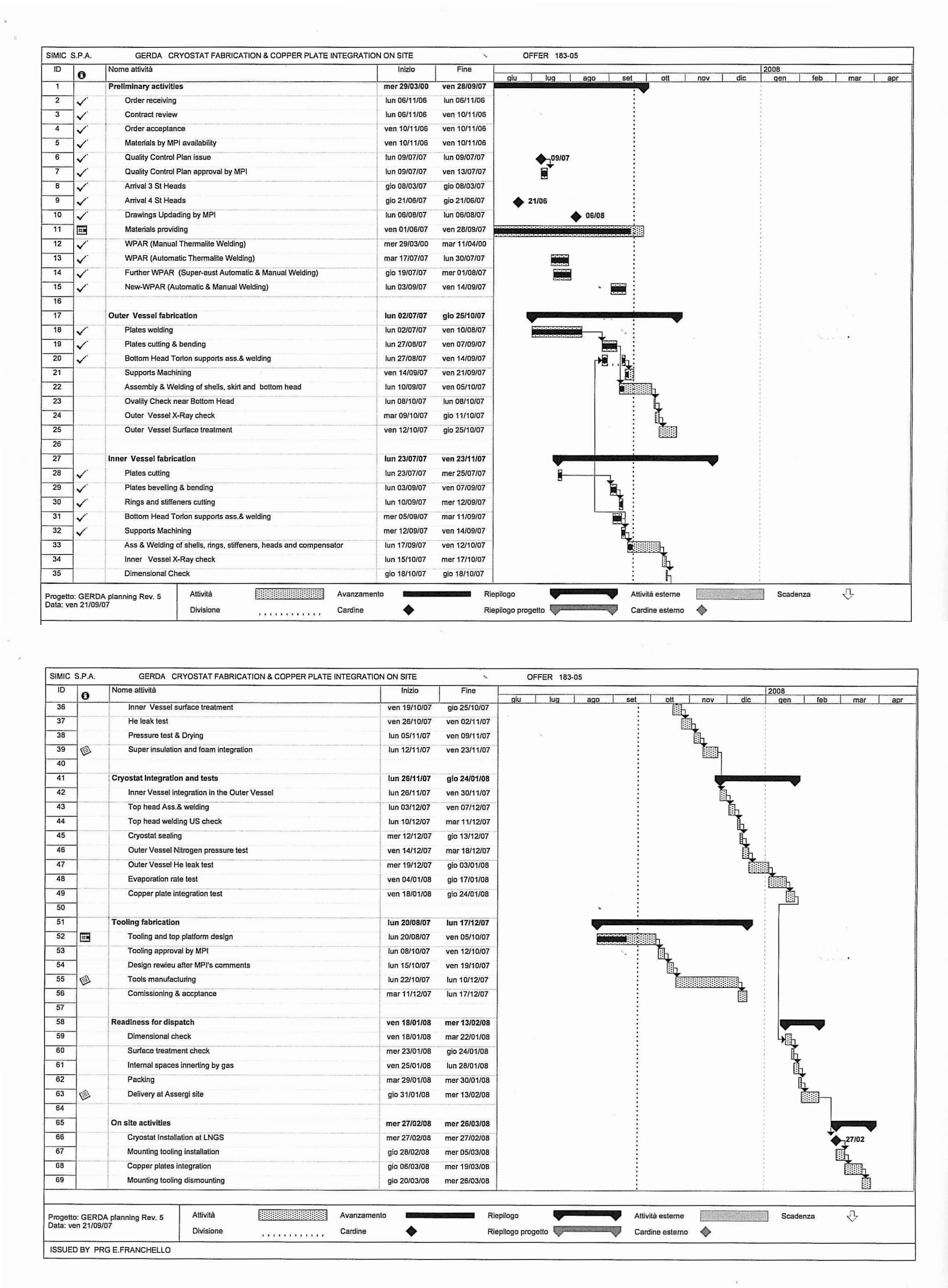

SIMIC S.P.A. GERDA CRYOSTAT FABRICATION & COPPER PLATE INTEGRATION ON SITE OFFER 183-05

ID	Nome attività	Inizio	Fine
1	**Preliminary activities**	**mer 29/03/00**	**ven 28/09/07**
2	Order receiving	lun 06/11/06	lun 06/11/06
3	Contract review	lun 06/11/06	ven 10/11/06
4	Order acceptance	ven 10/11/06	ven 10/11/06
5	Materials by MPI availability	ven 10/11/06	ven 10/11/06
6	Quality Control Plan issue	lun 09/07/07	lun 09/07/07
7	Quality Control Plan approval by MPI	lun 09/07/07	ven 13/07/07
8	Arrival 3 St Heads	gio 08/03/07	gio 08/03/07
9	Arrival 4 St Heads	gio 21/06/07	gio 21/06/07
10	Drawings Updading by MPI	lun 06/08/07	lun 06/08/07
11	Materials providing	ven 01/06/07	ven 28/09/07
12	WPAR (Manual Thermalite Welding)	mer 29/03/00	mar 11/04/00
13	WPAR (Automatic Thermalite Welding)	mar 17/07/07	lun 30/07/07
14	Further WPAR (Super-aust Automatic & Manual Welding)	gio 19/07/07	mer 01/08/07
15	New-WPAR (Automatic & Manual Welding)	lun 03/09/07	ven 14/09/07
16			
17	**Outer Vessel fabrication**	**lun 02/07/07**	**gio 25/10/07**
18	Plates welding	lun 02/07/07	ven 10/08/07
19	Plates cutting & bending	lun 27/08/07	ven 07/09/07
20	Bottom Head Torlon supports ass.& welding	lun 27/08/07	ven 14/09/07
21	Supports Machining	ven 14/09/07	ven 21/09/07
22	Assembly & Welding of shells, skirt and bottom head	lun 10/09/07	ven 05/10/07
23	Ovality Check near Bottom Head	lun 08/10/07	lun 08/10/07
24	Outer Vessel X-Ray check	mar 09/10/07	gio 11/10/07
25	Outer Vessel Surface treatment	ven 12/10/07	gio 25/10/07
26			
27	**Inner Vessel fabrication**	**lun 23/07/07**	**ven 23/11/07**
28	Plates cutting	lun 23/07/07	mer 25/07/07
29	Plates bevelling & bending	lun 03/09/07	ven 07/09/07
30	Rings and stiffeners cutting	lun 10/09/07	mer 12/09/07
31	Bottom Head Torlon supports ass.& welding	mer 05/09/07	mar 11/09/07
32	Supports Machining	mer 12/09/07	ven 14/09/07
33	Ass & Welding of shells, rings, stiffeners, heads and compensator	lun 17/09/07	ven 12/10/07
34	Inner Vessel X-Ray check	lun 15/10/07	mer 17/10/07
35	Dimensional Check	gio 18/10/07	gio 18/10/07
36	Inner Vessel surface treatment	ven 19/10/07	gio 25/10/07
37	He leak test	ven 26/10/07	ven 02/11/07
38	Pressure test & Drying	lun 05/11/07	ven 09/11/07
39	Super insulation and foam integration	lun 12/11/07	ven 23/11/07
40			
41	**Cryostat Integration and tests**	**lun 26/11/07**	**gio 24/01/08**
42	Inner Vessel integration in the Outer Vessel	lun 26/11/07	ven 30/11/07
43	Top head Ass.& welding	lun 03/12/07	ven 07/12/07
44	Top head welding US check	lun 10/12/07	mar 11/12/07
45	Cryostat sealing	mer 12/12/07	gio 13/12/07
46	Outer Vessel Nitrogen pressure test	ven 14/12/07	mar 18/12/07
47	Outer Vessel He leak test	mer 19/12/07	gio 03/01/08
48	Evaporation rate test	ven 04/01/08	gio 17/01/08
49	Copper plate integration test	ven 18/01/08	gio 24/01/08
50			
51	**Tooling fabrication**	**lun 20/08/07**	**lun 17/12/07**
52	Tooling and top platform design	lun 20/08/07	ven 05/10/07
53	Tooling approval by MPI	lun 08/10/07	ven 12/10/07
54	Design rewieu after MPI's comments	lun 15/10/07	ven 19/10/07
55	Tools manufacturing	lun 22/10/07	lun 10/12/07
56	Comissioning & accptance	mar 11/12/07	lun 17/12/07
57			
58	**Readiness for dispatch**	**ven 18/01/08**	**mer 13/02/08**
59	Dimensional check	ven 18/01/08	mar 22/01/08
60	Surface treatment check	mer 23/01/08	gio 24/01/08
61	Internal spaces innerting by gas	ven 25/01/08	lun 28/01/08
62	Packing	mar 29/01/08	mer 30/01/08
63	Delivery at Assergi site	gio 31/01/08	mer 13/02/08
64			
65	**On site activities**	**mer 27/02/08**	**mer 26/03/08**
66	Cryostat Installation at LNGS	mer 27/02/08	mer 27/02/08
67	Mounting tooling installation	gio 28/02/08	mer 05/03/08
68	Copper plates integration	gio 06/03/08	mer 19/03/08
69	Mounting tooling dismounting	gio 20/03/08	mer 26/03/08

Figure 10: Updated time schedule for cryostat production provided by manufacturing company SIMIC S.p.A..

Since September the production of the cyogenic vessel has acquired momentum and the following figures show examples of various manufacturing steps like machining of the supporting elements at the bottom head of the cryostat's inner container (Fig. 7, right), bevelling of the long steel sheets, or rolling of the cylindrical shell (Fig. 8).

The internal high purity copper shield has been produced and is stored since June underground at LNGS. It consists of 20 segments each assembled from two 3 cm thick copper plates of 0.615 m width and 2.40 m resp. 2.00 m height (Fig. 9, left). It is complemented by 20 further 3 cm thick shields of an area of 0.615 x 0.40 m^2, each. The copper plates have been rolled by CSN Schreiber, Neunkirchen, from OFRP copper produced by the Norddeutsche Affinerie, Hamburg. After rolling, the plates were warmed up to 50 °C and pickled in >15% sulfuric acid. Immediately afterwards, the plates were rinsed with deionized water. For transportation, the plates were vacuum-packaged (Fig. 9, right) and covered by an additional plastic wrap.

For the cryostat's cryogenic infrastructure a draft of the tender document has been prepared and submitted to an external consultant as well as to interested companies for comments. In parallel, suppliers of critical hardware parts like Rn tight valves have been identified. The tendering procedure is planned to start now in October.

7 Water tank and infrastructures

Major progress in the preparation of the main Gerda site includes the deployment of the 24 anchorages points for the fixation of the cryostat in June 2007 and the subsequent installation of the bottom plate of the Water Tank (WT) in Hall A in July 2007.

Figure 11 shows the Gerda main site as it is now: the WT bottom plate and the ring of anchorages for the fixation of the cryostat skirt are visible. The WT construction will resume after the arrival and tests of the cryostat. Starting from this moment, 12 working weeks are scheduled to complete the construction of the WT. The final test, which includes to fill the WT completely with water, is planned for summer 2008. The draining of the water from the WT for test, operation and emergency must still be defined and authorized by Lngs.

Lngs has officially assigned to the Gerda collaboration the locations for the LAr and LN storage tanks in the TIR tunnel within the Hall A containment.

The tender for the construction of the Technical Building (funded by Lngs) has been awarded and the contract has been signed. The work on site will start after the completion of the WT.

Since summer 2007 an experienced project engineer is working on site for the collaboration. The major ongoing activities include the review and design of the electric plants of the Gerda Technical Building, the elaboration of the specifications for the heater of the gas exhaust from the cryostat in case of an emergency event, and the definition of the water draining procedures for the final acceptance test of the WT, for the operation of the experiment and for the case of emergency.

Figure 11: Bottom plate of the water tank at the main GERDA site in Hall A of LNGS as of August 2007.

8 Muon veto

8.1 Cherenkov veto

As the principle design for the encapsulation has been determined, the emphasis was on quality control. The first two prototypes have sustained extensive tests for water tightness including pressure tests. The potentially weak point around the shrinking hose which replaces the very expensive Jupiter connector did not show any sign of leakage.

A preproduction assembly has been performed by building five complete PMT capsules (Fig. 12). Details have been learned to improve the timing within the production process. In particular different types of polyurethane have been tested to optimize filling and hardening times. The performance of the PMTs after encapsulation have been tested electronically with the data acquisition system which is now being prepared for the next tests with the plastic veto in Tübingen and at the GDL.

According to recent tests the water resistance of the VM2000 foil is good enough to allow the glue to remain on the backside of this reflector foil.

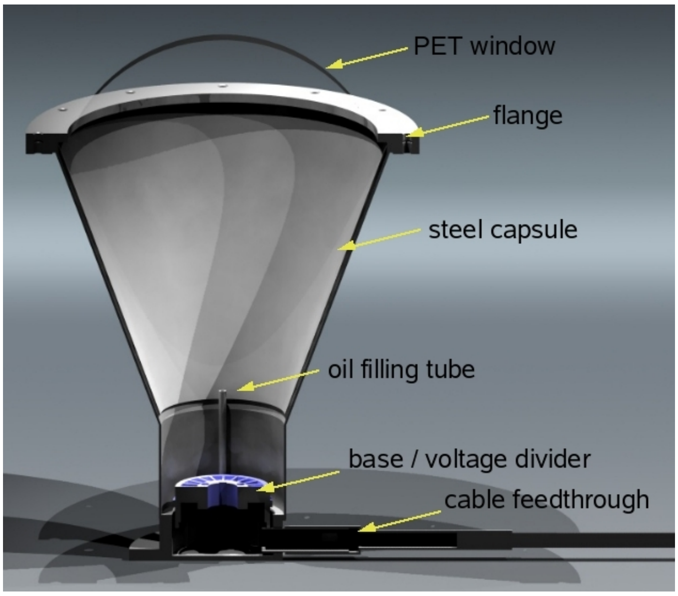

Figure 12: Schematic drawing of the stainless steel capsule to house the PMT for the water Cerenkov detector.

8.2 Plastic veto

A batch of 10 plastic scintillators with dimensions of $200\times50\times3$ cm^3 has been assembled and first tests have been performed.

The readout is performed via wavelength shifting fibers and Hamamatsu H6780 phototubes. An amplifier/shaper and discriminators are located directly at each base providing one analog and two logic outputs for the data analysis. The test showed that the concept works in principal, but more wavelength shifting fibers and green-extended H6780-20 phototubes are desirable for improved performance.

A shipment of about 10 units is planned as well as tests with the envisaged data acquisition system at Heidelberg and Tübingen.

9 Infrastructure on top of the tank

The upper infrastructural complex is sitting on the Gerda Technical Building. Its main constituent is the clean room which houses the lock system for insertion of the detectors to the cryogenic volume.

9.1 Clean room

The design of the clean room has been presented to the Scientific Committee before. Mechanical specifications and infrastructural requests to the Lngs are stable. The clean room is presently in the tendering process. The winner of the tender will be determined in November.

The storage system (Fig. 13) for the naked HPGe detectors has been assembled and tested. It allows for controlled flushing the detectors with dry gas while they are stored in their individual containers. For transport the containers can be evacuated. The system is ready for delivery to LNGS.

Figure 13: The storage system for naked HPGe detectors.

A prototype of the test stand that will be used to test the contacting of the phase II detectors after transport is currently being assembled.

9.2 Lock system

The main parts of the lock system are the inner and the outer lock as well as two cable tubes. The inner lock houses the rail system to position the detector strings in the array. The cable tubes contain the linear pulleys to lower individual detector strings to the cryogenic volume. The inner lock system can be decoupled from the cryostat with a circular shutter. Rectangular shutters separate the inner from the outer lock and the outer lock from the clean-room. The lock system is supported by steel bars that rest on the superstructure.

Inner rail system The rail system for the inner lock is shown in Fig. 14. It has been assembled and successfully tested using a gear wheel to move the cable car around the circular rail and a magnetic transfer arm to push the string from the circular rail to its final array position. Production and assembly of the final rail system is on its way.

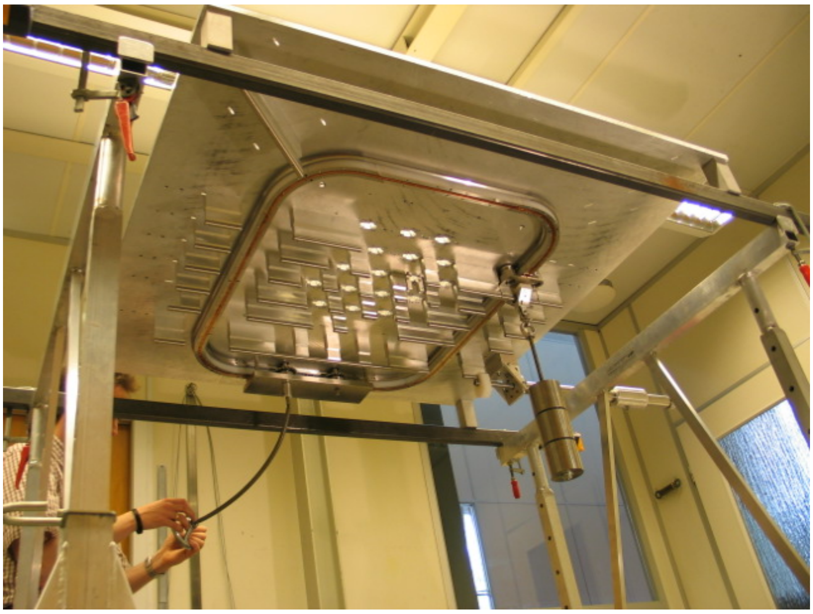

Figure 14: Mock up of the rail system in the inner lock.

Linear pulley system The angular position of the cable strings around its center has to be reproducible with a precision of $\pm$ 5°. During the lowering procedure no vibrations with displacements $\geq$ 10 mm and no rotational oscillations with amplitudes $\geq$5° are allowed. It was found that the rotational behavior of the strings does heavily depend on the type of the used cables and the implementation of guidance of the cables along the string. For a full phase I cabling including spare signal cables and HV cables the specifications have been met using a cable drag chain with selected Teflon sub-miniature micro-coaxial signal cables and Teflon unshielded HV cables.

The insertion of the detector strings for phase I and phase II to liquid argon has been tested. It could be demonstrated that the detector strings for phase I and phase II can be fully dipped into the cryo liquid within one hour without inducing rotation of more than $\pm$5° and oscillations with an amplitude of $\geq$10 mm. The engines for moving the individual strings are presently being ordered.

Shutters The shutters dividing the different components of the lock system have been assembled and individually leak tested at the site of the company. Fig. 15 shows pictures of the circular shutter and the rectangular shutters in the clean room area of VAT. They are presently being stored at the MPI für Physik in Munich.

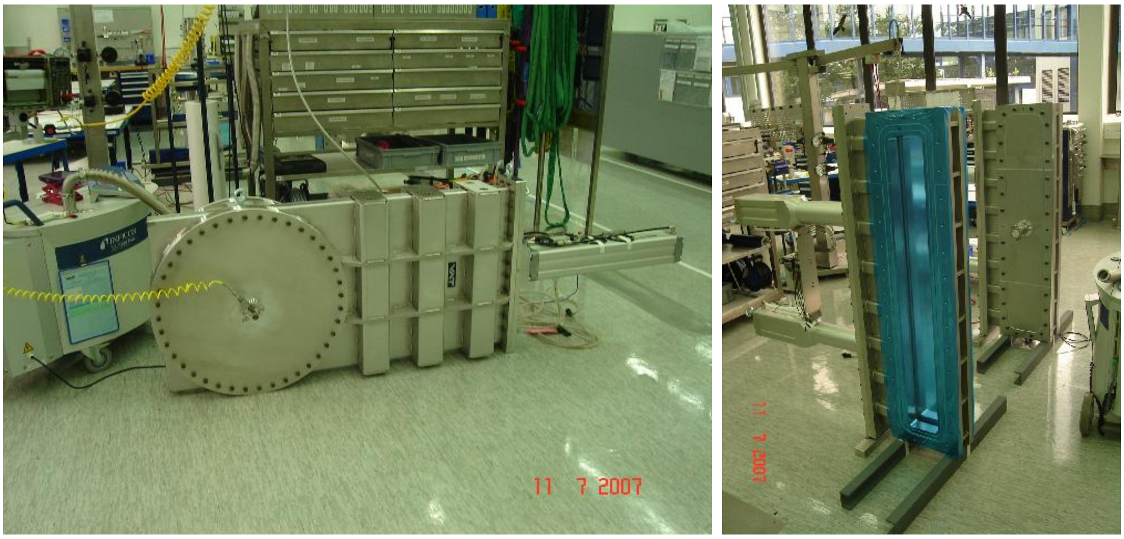

Figure 15: Vacuum shutters. Left: This circular shutter will separate the cryostat volume from the lock volume. Right: Rectangular shutters to separate the inner lock from the outer lock and the outer lock from the clean room.

10 Monte carlo simulations and background studies

The activity of the TG10 (Monte Carlo Simulations and Background Studies) in the past six months has been closely connected to other task groups, specifically TG1 (Phase I detectors), TG2 (Phase II detectors), TG6 (Muon veto) and TG11 (Material screening).

The group is continuously developing and maintaining the Geant4-based MaGe framework, together with the Majorana Monte Carlo group. A part of the recent activity was devoted to the code documentation in a complete User Manual and to the validation of the simulation physics results with test-stand data. A general paper about MaGe is in preparation.

The Gerda and Majorana Monte Carlo groups started the development of a new common interface, called MGDO (Majorana-Gerda data object), for the simulation of the detector pulse shapes. The interface allows data produced by MaGe simulations (namely, position, time and energy deposition of the hits) to be passed to external software packages that deliver the actual waveforms from the germanium detectors. In this way, the full simulation chain from primary particles to detector waveforms will be available. Different alternative algorithms for the waveform simulation (e.g. Agata one) are going to be implemented and tested.

Physics results from MaGe simulations have been compared to test-stand experimental data collected with the 18-fold n-type segmented detector in MPI-Munich. The detector has been exposed to γ-rays (^{60}Co, ^{228}Th and ^{152}Eu) and to neutrons from AmBe. The main results have already been included in the past reports to the Scientific Committee. Results with γ-rays show that the precision obtained in MaGe is better than 10% for full-energy peaks and about 5% for the Compton continuum. Results have been submitted to NIM A, and a preprint is available on arXiv [7].

Additional effort was devoted to analyze the differences between the simulated and experimental spectra from the AmBe neutron source. Though the simulation reproduces reasonably well the spectral shape (as shown in the previous Progress Report to the Scientific Committee, in April 2007), it has some spurious and/or missing peaks. During the last 6 months, some of the problems have been traced back to bugs or limits in GEANT4[2]. The bugs have been reported to the GEANT4 Collaboration. For some of them, an internal MAGE work-around has been developed. A paper describing the AmBe measurement and simulation is in preparation.

The Monte Carlo simulation task group works in close connection with other task groups. In particular, MAGE was used to simulate the experimental test-setup at the Gerda Detector Laboratory (GDL), for the interpretation of the leakage current measurements (see Sec. 2). The energy depositions by radioactive sources in the germanium crystal and in the "active" liquid argon region facing the passivation layer have been determined for different positions of the source.

Simulations are currently ongoing to estimate the muon-induced background (prompt and delayed) in the LArGe setup which is being built in the Gerda Detector Laboratory underground. Such a study is also meant to explore the possibility of the experimental measurement of the muon-induced neutron production with the LArGe setup.

The MAGE-based Monte Carlo simulation of the Cherenkov and plastic muon vetoes for GERDA has been recently improved by including details of the setup which were not essential for the first round of assessments. A revised evaluation of the efficiency of the Cherenkov and the plastic vetoes is going to be completed.

Since last year, MAGE has been used to derive the absolute efficiency of HPGe spectrometers used for material screening. Recently, a detailed description of the three HPGe spectrometers available at MPIK-Heidelberg has been fully implemented in the MAGE framework. The geometry model of the newest detector has been optimized by tuning the dead layer thickness and the inner hole size until the simulation results fitted the experimental data. In this context, a systematic check of the γ-ray branching ratios for radioactive decays in GEANT4 has been performed, resulting in the identification of three previously-unknown bugs in GEANT4. The bugs have been internally fixed and reported to the GEANT4 Collaboration.

Similarly, MAGE simulations were run for a new detector setup for material screening in HADES, in order to better understand and quantify the muon-induced background for underground screening measurements. Comparison of simulations to experimental results is ongoing.

[2]For instance, the fact that the GEANT4 neutron capture process is not able to produce isomeric states of the daughter nuclei, as ^{71m}Ge and ^{75m}Ge.

11 Material screening

11.1 ^{222}Rn emanation measurements

Radon emanation studies have been continued in the period under review. Tests on the Kalrez gaskets (10 batches) to be used in the shutter valves have been finished. The expected contribution to the overall radon budget in the lock coming from that source is estimated to be below 0.6 mBq. Measurements of 5 complete HV feed-throughs and 5 HV connectors resulted in (40 ± 14) μBq and (0.37 ± 0.07) mBq, respectively. The emanation rate of a magnetic arm (internal part) foreseen for the lock was found to be (0.24 ± 0.02) mBq. WEKA, KÄMMER and WTA cryogenic valves were tested in different configurations (gaskets, connection ports). For the first two (KÄMMER is completely metal sealed, WEKA has a butyl O-ring against atmosphere and a Teflon stamp seal) rates at the level of 50-80 μBq were obtained, while for the third one $\sim$ 2 mBq was found. Connection flanges of the WTA valve were sealed with Teflon and the stamp was fixed to the housing using a so-called Kammprofil gasket. Usage of different sealing materials here is still under consideration (measurements are ongoing). Diffusion tests (diffusion through seals of valve stamps) conducted for the WEKA and KÄMMER valves showed that they are tight against atmospheric radon. Measurements performed for the oxygen adsorber TRIGON (copper oxide on a alumina support) at room temperature resulted in a specific emanation rate of (0.49 ± 0.01) Bq/kg. Preliminary results obtained for 150 ^{o}C did not show any significant change (emanation tests at liquid argon/nitrogen temperature are planned). Finally, an emanation measurement on a coaxial cable (Habia) also shows a low radon production of (0.35 ± 0.08) mBq/kg measured on a 514g cable sample.

11.2 ^{222}Rn in argon

The search for argon with a low ^{222}Rn concentration was continued by (a) checking the purity of argon from different suppliers, (b) investigating the ^{222}Rn emanation of cryogenic storage tanks and (c) testing the performance of ^{222}Rn adsorber columns filled with activated carbon.

The initial ^{222}Rn concentration in technical quality argon from different Italian and German suppliers was found to be in the range of 0.5 mBq/m^3. This is lower than earlier measurements suggested, but still higher than the ^{222}Rn contamination in technical nitrogen. The systematic difference can be explained by the lower boiling point of nitrogen with respect to argon. Since radon has the highest boiling point, its segregation from nitrogen is more effective than from argon. In practice, the ^{222}Rn concentration is often determined by the emanation of the cryogenic storage tanks only. In the past we found widely spread ^{222}Rn emanation rates (from few mBq up to 180 mBq). The 6.3 m^3 LAr storage tank at Gran Sasso from where the argon for the phase I prototype testing is taken is by chance the purest storage tank we have ever measured (if scaled to its volume). Its emanation rate of (3.5 ± 0.2) mBq in saturation can well explain the low ^{222}Rn concentration (< 0.02 mBq/m^3 (STP)) which we found for argon stored for many weeks in that tank.

Within GERDA pure argon must be available without waiting for the decay of the initially present ^{222}Rn. Also argon might be re-contaminated by oxygen adsorbers (if they have to be used in GERDA) which emanate a lot of ^{222}Rn (see above). In both cases it is important to purify argon from ^{222}Rn. We have shown that cryo-adsorption of ^{222}Rn on activated carbon is a powerful purification technique for argon. Best results were obtained in the gas phase, but liquid phase adsorption (as required for GERDA) is also possible, although the efficiency is lower. Tests with a 60g activated carbon trap showed that reduction factors in the range of 10-100 can be obtained at argon flow rates of 15m^3/h (STP) and cooling temperatures between -166 ^{o}C and -180 ^{o}C. Ongoing tests with a 5 liter column that can be filled with varying amounts of activated carbon will help to improve the understanding of the liquid phase adsorption process. Eventually, this knowledge will be used to construct an argon purification plant dedicated for the requirements of GERDA.

11.3 γ ray screening

Screening of construction materials for GERDA by γ ray spectroscopy has been continued. Since the low-level laboratory of the MPIK Heidelberg is currently renovated and since the HPGe detectors at INR Baksan had to be repaired (see Sec. 11.5), these measurements have been conducted mainly at IRMM Geel and LNGS Assergi.

Before the renovation of the Low-level laboratory at MPIK Heidelberg had started, 2 materials relevant for the cryostat construction have been screened there by γ ray spectroscopy: a 1.0 kg sample of the Super-insulation foil needed as thermal insulation between the 2 cryostat walls, and a 12.9 kg sample of Makrolon which is applied to mitigate the consequences of a possible leak in the inner or outer container. All resulting activities (in most cases upper limits) are well below the required levels.

IRMM Geel has performed radiopurity measurements in the underground laboratory HADES (-225 m) using ultra low-background HPGe-detectors. The following samples have been measured in the period under consideration. (1) 800 pogo pins that should be free of CuBe2 were measured for 35 days. This new batch of pogo pins turned out to be better than the previous one, which contained CuBe2. The improvement (mainly in Th and ^{40}K) was, however relatively limited ($\sim$25%). (2) A Teflon coated high voltage cable was measured for 15 days. A second measurement which is still ongoing was requested in order to decrease the detection limits (or alternatively quantify the radioimpurities). (3) NOMEX Yarn was measured for 22 days, and (4) a set of transistors was measured for 14 days (also still ongoing).

At LNGS Assergi, the following measurements have performed by means of γ ray spectroscopy with HPGe detectors in the period under review: (1) coax cable Vaqtech, 1-CC-0712, 50 Ohm, silver plated copper wire, Kapton insulated; (2) coaxial cable Vaqtech, 1-CC-0710, 0.25 mm silver plated copper wire, Kapton insulated with braided shield (measurement ongoing); (3) coaxial cable Axon, silver plated copper wire, as used in the ATLAS experiment; (4)coaxial cable Habia; (5) Cuflon (copper plated PTFE) from Polyflon, for making circuit boards (also measured by ICP-MS); (6) concrete from the reinforced floor in hall A of the LNGS; (7) Ultraplan MAXI from MAPEI, self-levelling material for foundations of the GERDA experiment in hall A of the LNGS; and (8) IG21 from Fassa Bortolo, used for foundations of the GERDA experiment in hall A of the LNGS.

A large part of the time for γ ray screening in the period under review has been devoted to cables and their base materials, as can be seen from the measuring lists above. Table 4 summarizes these measurements. The best limits so far have been obtained for the Habia coaxial cable (line 5 in Table 4). This cable would be suited for GERDA phase I. The ^{222}Rn emanation rate measured for this cable can be converted into a specific ^{226}Ra activity under the reasonable assumption that the ^{222}Rn emanates fast enough. The resulting number, (0.35 ± 0.08) mBq/kg is a factor of 5 below the limit given in Table 4.

Some of cable samples contain the long-lives isomers ^{108m}Ag ($T_{1/2}$ = 418y) and ^{110m}Ag ($T_{1/2}$ = 250d). Of special concern is ^{110m}Ag since its Q value is above 2 MeV. However, the specific activity measured for instance for the Habia coaxial cable (1.3 ± 0.2 mBq/kg) is still acceptable.

Cable sample	**Specific activity [mBq/kg]**					
	^{228}**Th**	^{228}**Ra**	^{226}**Ra**	^{40}**K**	^{108m}**Ag**	^{110m}**Ag**
Cuflon	< 7.2	< 6.5	< 9.3	61 ± 16		
Teflon coated HV cable	< 8.0	< 8.0	< 2.5	56 ± 12	1.8 ± 0.3	9.0 ± 2.0
ATLAS Axon	< 12	< 15	< 12	230 ± 60	6.6 ± 2.1	
1-CC-0712 (50 Ohm)	< 11	< 8.0	< 11	610 ± 80	5.0 ± 1.2	
Habia Teflon Subm.	< 4.7	< 6.9	< 1.8	400 ± 40	0.78 ± 0.24	1.3 ± 0.2
Caburn 1-CC-0710	< 11	< 15	< 12	< 100		
Kapton flat cable	< 4.0		9 ± 6	130 ± 60		

Table 4: γ ray screening results for cables from different sources and of different design.

11.4 ICPMS measurements

An extensive study on U, Th and K concentrations in different samples consisting of polymeric substrates with metallic cladding by means of an Inductively Couplet Plasma Mass Spectrometer (ICP-MS) has been performed at LNGS. Basically two different types of samples were analyzed: (1) Different thickness of Teflon substrates with Cu cladding; (2) Kapton substrates without metallic cladding and with the following claddings: Cu; Cu and Ni; Cu, Ni and Au.

The results, expressed in terms of specific activities for ^{232}Th, ^{238}U and ^{40}K are presented in Table 5. It turns out that Kapton samples are significantly dirtier than Teflon samples. There is a difference of an order of magnitude or more in the U contamination, whereas for Th the difference is within is a factor of 5. Moreover it turns out that the contamination for Kapton samples mainly comes from the polymeric substrates since the contamination levels measured in the substrate without metallic cladding are similar to those measured in samples with claddings made of different metals.

Sample	**Specific activity [mBq/kg]**		
	^{232}**Th**	^{238}**U**	^{40}**K**
Kapton	0.6 ± 0.2	12 ± 4	9 ± 2
Kapton with Cu	$0.73\,^{+0.12}_{-0.08}$	$2.9\,^{+0.4}_{-0.3}$	< 22
Kapton with Cu + Ni	0.5 ± 0.1	12 ± 1	< 25
Kapton with Cu + Ni + Au	0.7 ± 0.1	2.0 ± 0.5	< 27
Cuflon 0.010 inch	0.20 ± 0.04	0.62 ± 0.12	< 30
Cuflon 0.015 inch	$0.28\,^{+0.04}_{-0.03}$	$0.36\,^{+0.07}_{-0.04}$	$5\,^{+9}_{-2}$
Cuflon 0.031 inch	$0.12\,^{+0.05}_{-0.04}$	$0.50\,^{+0.14}_{-0.12}$	< 25

Table 5: ICPMS results on different Kapton and Cuflon samples

11.5 Low-level instrumentation

Irmm Geel installed a new HPGe-detector system based on a sandwich configuration. This detector system has a muon shield and two HPGe-detectors and will offer measurements with improved sensitivity for small samples.

At Inr Baksan, the four Igex-Baksan HPGe detectors have been continously operated for more than 14 years. They have been pumped only once in this long period. During the last year an increase of the noise level has been observed for the 3 enriched Igex detectors which most probably was due to a distortion of the vacuum level. Therefore it has been decided to dismount the whole 4 HPGe set-up, to check the vacuum and to pump the 3 Igex detectors. As a result the noise level of all 3 detectors returned to the previous working conditions (less than 10 mV). The fourth non-enriched detector was not pumped because it still works perfectly.

In addition, it was decided to modify and renew the electronics and DAQ system, which has been in use without interruptions and modifications since 1993. This work has been finished recently. Currently a background measurement is under way which will last for 1 to 2 months. After that the 4 HPGe spectrometer will be ready to continue material screening for Gerda.

In the previous progress report a ^{207}Bi contamination in the newly constructed GeMpi III spectrometer at Lngs was mentioned. This contamination has been located within the cryostat. Furthermore, it turned out that another new detector at Lngs, GeMpi IV also suffers from such a contamination, although lower by a factor of about ten. A cross-contamination coming from a ^{207}Bi-solution via tools from an allegedly clean toolbox has been identified as the reason. By the end of July a cleaning attempt was conducted on GeMpi IV, dismounting and acid cleaning the cryostat part by part. Preliminary background data revealed a reduction of the contamination by a factor of three to four. Further steps will be decided when background data with better statistics are available.

The determination of the counting efficiency for sample screening by means of γ ray spectroscopy is often based on MC simulations of the detector and sample geometry. In order to improve this procedure for the Corrado detector at Mpik Heidelberg, an optimization of the geometrical model for this detector was performed. The external dimensions and the position of the crystal have been determined earlier by X-ray screening. The remaining parameters to be determined were the thickness of the dead layer and the size of the inner hole. This was done by measuring several low- and high-energy γ ray sources and by comparing the results with simulations carried out with different parameter settings, until a good fit with the data was found. The preliminary optimized geometry of Corrado was then used in the evaluation of the NPL Proficiency Test Exercise 2007, in which the Mpik Heidelberg participated. However, the recently obtained results of this intercomparison indicate that the anticipated accuracy of <6% has not been reached yet. Therefore a second, more systematic optimization cycle is currently under way.

11.6 Radon monitoring

The chamber intended to monitor the ^{222}Rn concentration in the air of the Gerda detector setup at Lngs is currently tested at Mpik Heidelberg. This monitor is similar to the one used in Borexino [8]. Improvements as compared to the last progress report have been achieved with respect to background event reduction. The inner surfaces of the detector were cleaned with a special water vapor treatment. Further, the double amplifier technique [9] was applied in order to identify signals produced by high voltage discharges and possibly cosmic ray events. A hardware logic board discriminates such signals with a shape analysis before the events are recorded by a multichannel analyzer. The monitor works now with a high voltage of 50 kV instead of 35 kV which increases the sensitivity. The ^{222}Rn concentration of air samples is calculated from the activity of the collected Polonium ions. However, the collection efficiency for positive ions in the ^{222}Rn decay chain depends on the concentration of water and other molecules in the air. The behavior of the chamber on these pollutions has to be measured. According to an evaluation procedure described in [8] the ^{222}Rn concentration can be corrected for the reduced collection efficiency. It is planned to perform this study and the calibration of the chamber with a known ^{226}Ra source in the near future.

References

[1] M. Barnabé Heider, O. Chkvorets, S. Schönert, C. Cattadori, K. Gusev, M. Shirchenko, Measurements of the leakage current of a phase I prototype detector operated in liquid argon in response to gamma radiation, GERDA Scientific Technical Report GSTR-07-005 (2007).

[2] C. Cattadori, A. Di Vacri, L. Pandola, M. Barnabe-Heider, O. Chkvorets, S. Schönert, Notes on the reverse current dependence of a naked Ge crystal operated in liquid argon on the ionization rate of the surrounding liquid argon. GERDA Scientific Technical Report GSTR-07-009 (2007)

[3] S. Belogurov, L. Bezrukov, L. Inzhechik, I. Kirpichnikov, B. Lubsandorzhiev, Design of Naked HP Ge Detector for Operation in LAr, GERDA Scientific Technical Report GSTR-07-011 (2007)

[4] I. Abt *et al.*, 'Test of pulse shape analysis using single Compton scattering events', arXiv:0708.0917; I. Abt *et al.*, 'Pulse shapes from electron and photon induced events in segmented high-purity germanium detectors', arXiv:0704.3016; I. Abt *et al.*, 'Background reduction in neutrinoless double beta decay experiments using segmented detectors - a Monte Carlo study for the GERDA setup', Nucl. Instr. Meth. A 570 (2007) 479-486; I. Abt *et al.*, 'Identification of photons in double beta-decay experiments using segmented germanium detectors - studies with a GERDA Phase II prototype detector', nucl-ex/0701005; I. Abt *et al.*, 'Characterization of the first true coaxial 18-fold segmented n-type prototype detector for the GERDA project', Nucl.Instrum.Meth. A 577 (2007) 574.

[5] GERDA coll., Progress Report at the LNGS Scientific Committee,LNGS-EXP 33/05 add. 3/06

[6] A. Pullia, F. Zocca, C. Cattadori, Low-noise amplification of gamma-ray detector signals in hostile environments IEEE TRANS NUCL SCI, vol. 53, no. 3, pp. 1744-1748 (2006)

[7] I. Abt *et al.*, Identification of photons in double beta-decay experiments using segmented germanium detectors - studies with a GERDA Phase II prototype detector, submitted to Nucl. Instr. and Meth. A, preprint arXiv:nucl-ex/0701005v1 (2007)

[8] J. Kiko, Nucl. Inst. Meth. A 460 (2001) 272-277.

[9] J. Kiko, Nucl. Inst. Meth. A 482 (2002) 434-440.